

# Sterol Uptake by an Alkali- $\beta$ -Cyclodextrin Metal-Organic Framework

Barry A. Blight,<sup>\*a,b</sup> Towseef I. Ahmad,<sup>b</sup> Helena J. Shepherd,<sup>b</sup> Christopher S. Jennings,<sup>a</sup> Livia I. Ferland,<sup>a</sup> Simon J. Teat<sup>c</sup> and Jeremy S. Rossman<sup>\*d</sup>

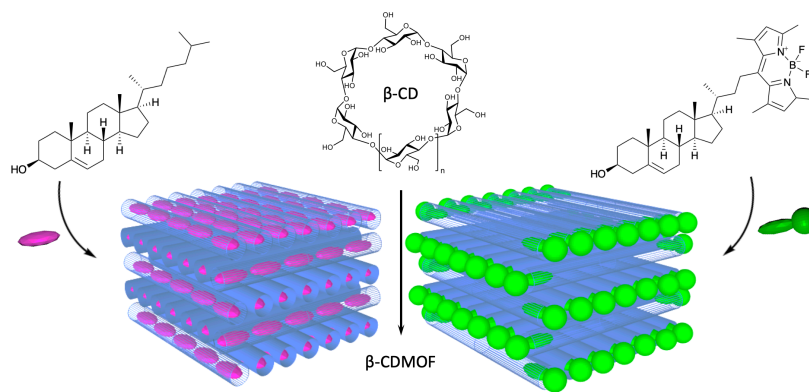
<sup>a</sup>Department of Chemistry, University of New Brunswick, Fredericton, N.B., E3B 5A3, Canada

<sup>b</sup>School of Physical Science, University of Kent, Canterbury, CT2 7NH, United Kingdom

<sup>c</sup>Advanced Light Source, Lawrence Berkeley National Lab, Berkeley, CA 94270, USA

<sup>d</sup>School of Bioscience, University of Kent, Canterbury, CT2 7NH, United Kingdom

KEYWORDS: coordination networks, metal-organic frameworks, cyclodextrin, cholesterol, organic molecule absorption



**Abstract:**  $\beta$ -Cyclodextrin is well known in cellular biology for its ability to moderate cholesterol levels in lipid bilayer membranes. Its use in extended network solids remains elusive due to the low symmetry of this macrocyclic system. Self-assembly of two different  $\beta$ -cyclodextrin MOFs with extended nanotube structures is achieved by crystallization with excess potassium hydroxide, one in the presence of cholesterol. We then further demonstrate the proclivity of one of these MOFs to absorb cholesterol and two other sterols from solution using NMR and confocal microscopy techniques. This work demonstrates that these network solids show great potential in both substrate delivery and/or extraction.

Cyclodextrins (CDs) are a unique class of material with uses spanning the biological, chemical and materials sciences. The three most common forms of CD are comprised of six ( $\alpha$ -), seven ( $\beta$ -), and eight ( $\gamma$ -) 1,4-linked pyranose units giving rise to cylindrical-shaped structures with hydrophilic exterior and a hydrophobic core. Their unique three-dimensional shape offer materials scientists several chemical handles for functionalization, and predictable behaviour with the primary and secondary faces of the toroid pointed with equatorially disposed glycosidic 1,3- and 1,2-diols, respectively (Figure 1).<sup>1-4</sup> Ideally positioned for meta-ligand chelation, the development of coordination networks that incorporate the toroidal motif in a manner that gives rise to extended ordered porosity has received notable interest in recent years.<sup>5</sup> While there is still substantial untapped promise in the use of these sugar-centric network solids (also referred to as metal-organic frameworks; in this case CD-MOFs), to date they have demonstrated limited success beyond carbon dioxide uptake,<sup>6,7</sup> gold ion extraction,<sup>8,9</sup> separating small chiral / aromatic compounds,<sup>10,11</sup> and mediated drug release.<sup>12,13</sup> This is in contrast to myriad of other applications that now employ multi-topic carboxylate-linked MOFs including but not limited to gas-sorption/separation,<sup>14,15</sup>

water sorption,<sup>16</sup> catalysis,<sup>17</sup> sensing,<sup>18,19</sup> and drug delivery.<sup>20,21</sup> Few of these systems, however, are derived entirely from renewable or naturally available components,<sup>22–26</sup> making the pursuit of CD-based MOFs with demonstrable utility particularly important. While the components of CD-based MOFs would be considered naturally occurring and/or derived from renewable resources, very few have demonstrated usefulness within -or interacting with components of- the biological arena.<sup>12,27</sup> We found this particularly intriguing considering the important role that  $\beta$ -CD plays in biochemical research. It has been well documented that  $\beta$ -CD and by extension, methyl- $\beta$ -CD (MBCD) have become quintessential tools in the mediation of intralamellar cholesterol levels from outside the membrane environment in order to influence cholesterol-dependent cellular processes.<sup>28</sup> For example, MBCD has been used to treat tissue culture cells to control cholesterol-dependent budding of influenza viruses,<sup>29</sup> and was separately demonstrated to modulate cholesterol interaction with the in-membrane oxytocin receptor protein.<sup>30</sup> In parallel and of particular importance in medical research, is the study of  $\beta$ -CDs as potential lipoprotein mimics by moderating in vivo cholesterol metabolism for combating atherosclerosis.<sup>31–33</sup> Through the formation of a [n]pseudorotaxane-style host-guest (HG) inclusion complex, hydrophilic  $\beta$ -CD solubilizes the highly hydrophobic sterol (and others) in aqueous environments with a remarkable association constant of  $K_a = 1.7 \times 10^4 \text{ M}^{-1}$ , as determined by the spectral displacement method.<sup>34</sup> In fact, this is such an effective solubilizing system that a  $\beta$ -CD-cholesterol HG-complex is commercially available from a number of suppliers as ‘Cholesterol Water Soluble’.

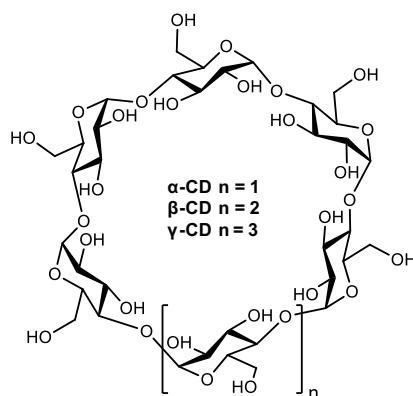


**Figure 1.** General structure of the three most common commercially available cyclodextrins.

In this account, we report the self-assembly of two new  $\beta$ -cyclodextrin-centered MOFs with apertures that align to form extended nanotubular arrays; one of which includes full characterization due to its broader HG applications ( $\beta$ -CDMOF-1) comprised of  $\beta$ -CD and  $K^+$ . Separately, crystalline  $\beta$ -CDMOF-2•Chol was grown in the presence of cholesterol and structure confirmed by single crystal XRD, a first for this particular HG complex as an extended network and only the second time as a discrete HG complex.<sup>35</sup> This is surprising considering the ubiquitous use of the  $\beta$ -CD-cholesterol complex in biology and across multiple divisions of chemistry.<sup>36,37</sup> Second, we demonstrate that ( $\beta$ -CDMOF-1 is capable of extracting cholesterol (along with other sterols) from solution into the extended network pores of the sugar-based nanotube structures, and further examine the crystal sponge behaviour by BODIPY-labelled cholesterol and separately resorufin uptake by fluorescence microscopy.

Self-assembly of  $\beta$ -CDMOF-1 and -2•Chol was achieved by slow solvent diffusion (either vapour or layering as noted) of methanol into combined aqueous solutions of  $\beta$ -CD (1.0 eq.) and potassium hydroxide (KOH; 20 eq.) in the presence or absence of desired the guest species. Crystal growth of described topologies was highly reproducible, and achieved within a 5-day timeframe.

Inspired by the works of Stoddart and coworkers,<sup>26</sup> we began the studies by attempting to assemble the networks with potassium hydroxide. The challenge with crystallizing any extended arrays of  $\beta$ -CD would be the decreased symmetry due to the  $C_7$ -rotational symmetry of  $\beta$ -CD.

$\beta$ -CDMOF-1 crystallized in Triclinic  $P1$  space group as colorless plates that grow from a central point, resulting in starburst-shaped crystal clusters in an 83% yield. The asymmetric unit is comprised of four crystallographically distinct  $\beta$ -CD toroids, which form cylindrical nanotubes through head-to-head / tail-to-tail complimentary H-bonding interactions between primary and secondary alcohol moieties on each rim of the molecules. The nanotubes are linked together into 2-dimensional sheets of parallel nanotubes, and adjacent sheets are aligned at  $95^\circ$  to one another through coordination of nine crystallographically unique potassium ions. The porosity of this structure thus extends infinitely along the a- and b-axes in discrete channels through the interior of the  $\beta$ -CD channels, as shown in Figure 2.

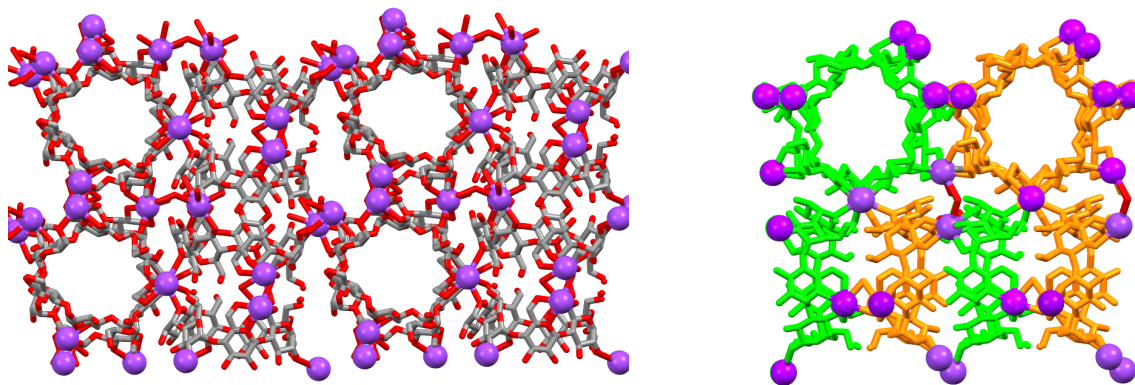


**Figure 2.** Two separate visualisations of  $\beta$ -CDMOF-1. Left: expanded view of network lattice; Right: condensed view of network lattice with colored  $\beta$ -CD rings to demonstrate topological alignment. In both images, hydrogen atoms and water molecules are removed for clarity. Potassium, purple; carbon, grey; oxygen, red.

Volatility of the methanol supernatant resulted in rapid solvent loss of the crystals and disintegration of the crystal lattice. Removal of the supernatant and soaking in ethanol for 24 hours followed by two 24-hour dichloromethane soaks afforded starburst crystals stable enough to be easily handled for TGA, elemental analysis, and X-ray powder diffraction (see supporting information). In fact, the DCM soaking protocol was demonstrated by TGA to slightly increase the thermal stability of the coordination assembly (See SI, Fig. S3), though any solvent loss adversely affected the extended crystallinity of the material as seen in the X-ray powder diffraction. Porosimetry experiments were unsuccessful, as the material was not stable enough to withstand the activating conditions required. Nonetheless, surface area was estimated using low level Connolly Surface calculation to be  $1250 \text{ m}^2\text{g}^{-1}$ , using the single crystal diffraction data. When the material remained solvated, however, the crystals remained intact and could be easily handled and transferred between vessels.

$\beta$ -CDMOF-2•Chol crystallized as colorless cuboid crystals in a Monoclinic  $P2_1$  space group with  $\beta$ -CD units aligned to form parallel one-dimensional nanotubes, with primary and secondary faces of the CD toroids again assembled in a head-to-head / tail-to-tail arrangement, stabilized by several complimentary H-bonds at each interfacial junction. Three potassium ions (one of which is partially occupied) participate in inter-nanotube coordination, forming a network of parallel nanotubes along the unit cell's  $a$ -axis. The pores of these tubes contain guest cholesterol molecules (1/3 occupancy for each pair of CD host molecules; thus 1:6 cholesterol/ $\beta$ -CD ratio), which have been crystallographically characterized in-situ, as shown in Figure 3. The observation of cholesterol within the pores suggests that these networks may be capable of cholesterol uptake in the form of a crystal sponge.<sup>38</sup> Considering that the conditions for assembly of  $\beta$ -CDMOF-2•Chol mirrored that of  $\beta$ -CDMOF-1, we posit that the presence of cholesterol contributed in the

templating of the parallel one-dimensional porous network, an attribute we are currently exploring. Investigation of the structure reveals no significant intermolecular interactions between any cholesterol functionality and the interior walls of the CD channels. Specifically to this structure, we see no hydrogen bond contacts to the free secondary alcohol of cholesterol by any  $\beta$ -CD oxygen. As this is a coordination network and not a solvated intermolecular HG system, the two environments are not comparable but this observation supports conclusions that a driving force for the solvated HG assembly is predominantly by solvophobic Van der Waals' attraction.

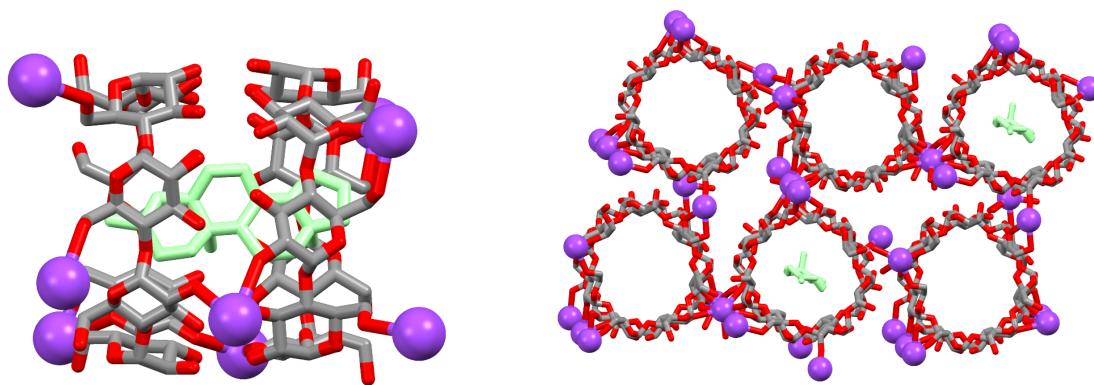


**Figure 3.** Visualization of  $\beta$ -CDMOF-2•Chol containing one-third cholesterol occupancy. Left: asymmetric unit exhibiting guest binding of cholesterol within the  $\beta$ -CDMOF pores, looking down c-axis; Right: expanded view of the lattice network looking down the b-axis. Hydrogen atoms, water molecules, and the disordered cholesterol alkyl-chain are removed for clarity. Potassium, purple; carbon, grey; oxygen, red; cholesterol, green.

To examine the uptake of molecular cholesterol from solution, we first chose to establish the stability of the crystal morphology during the cholesterol soaking process compared to ‘free’ crystalline  $\beta$ -CD. Soaking of  $\beta$ -CD crystals in an ethanolic solution of cholesterol resulted in the visible crystallization of cholesterol on the surface of the non-porous close-packed  $\beta$ -CD solid

(See SI, Fig. S5). Single crystal diffraction analysis of these hybrid crystals revealed a single crystal pattern indistinguishable from that of  $\beta$ -CD, superimposed with a powder diffraction pattern of cholesterol originating in the crystallites that had grown on the surface. This indicates that cholesterol does not penetrate into  $\beta$ -CD crystals, rather interacting with the surface only. However, soaking of  $\beta$ -CDMOF-1 under the same conditions resulted in unchanged crystal morphology, presumably because the network solid is being loaded with cholesterol instead of nucleating on the surface.

$^1\text{H}$  NMR analysis of the digested solids followed to assess this behaviour. Again, crystals of  $\beta$ -CDMOF-1 were soaked in an ethanolic solution of cholesterol for 24 hours, the supernatant removed, and crystals rinsed twice to dissolve away any surface adsorbed cholesterol with remaining solvent being removed in-vacuo. The  $\beta$ -CDMOF-1 solids were then digested in the chosen NMR solvents to assess host-guest ratios in identifying degree of cholesterol uptake. This analysis revealed an approximate ratio of 2:1  $\beta$ -CD to cholesterol (Figure 4a) by integration of the respective  $^1\text{H}$  NMR signals. We surmise that this ratio is too large to be merely surface adsorption of cholesterol to the crystal surface (particularly after a rinsing protocol), nor do we feel any accessible crystal fracture planes would accommodate cholesterol due to the highly ionic nature of the adjoining space between the nanotubular arrays. This study was also extended to include deoxycholic acid,  $\beta$ -estradiol, and a size-comparable dye molecule named resorufin (Figure 4b). The two related sterols showed similar uptake capacities (3:1  $\beta$ -CD to deoxycholic acid and 14:1  $\beta$ -CD to  $\beta$ -estradiol; see SI, Section 6) establishing that  $\beta$ -CDMOF-1 does indeed demonstrate crystal sponge behaviour. The root cause of this host-guest interaction is largely driven by solvophobic effects due to high polarity of the ethanol solvent and low polarity of the  $\beta$ -CD nanotubes. This is comparable to the complexation of free  $\beta$ -CD or MBCD with cholesterol in



water (a well-documented system).<sup>34</sup> In contrast, we see no uptake of resorufin by NMR analysis, for which we attribute this to its smaller size (fewer Van der Waal's interactions) and much higher localized polarity.

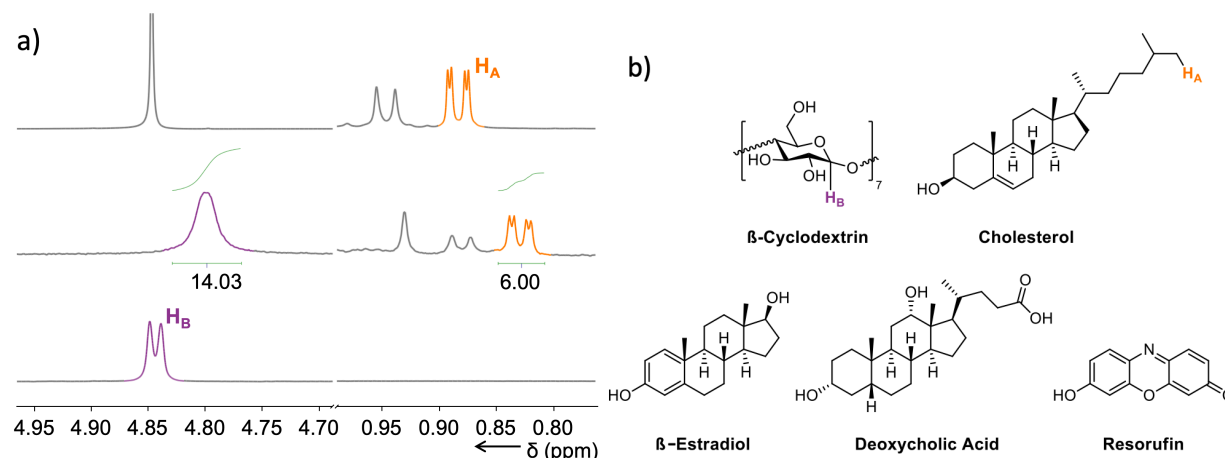


**Figure 4.** (a) Selected peaks from the <sup>1</sup>H NMR spectra of cholesterol (methanol-d<sub>4</sub>, 400 MHz, top) cholesterol-soaked β-CDMOF-1 (digested in methanol-d<sub>4</sub>/ DMSO-d<sub>6</sub>, 400 MHz, middle) and β-CD (methanol-d<sub>4</sub>/ DMSO-d<sub>6</sub>, 400 MHz, bottom). Full spectra shown in Fig. S6 (see SI). (b) Molecular structures of β-CD and sterol guest molecules in this study. Proton environments that give rise to the peaks in Fig. 4a are highlighted for β-CD (purple) and cholesterol (orange).

Since <sup>1</sup>H NMR is not direct evidence of cholesterol uptake, and SCXRD on cholesterol-soaked crystals afforded pore contents of intractable disorder, further evidence of this phenomenon was collected using fluorescence confocal microscopy, by employing guest molecules containing strongly emitting fluorophores (Figure 5). To accomplish this, we chose to employ commercial Bodipy-cholesterol (BO-C), which is as the name suggests, a Bodipy-conjugated cholesterol commonly used in cell imaging,<sup>39</sup> and separately, the aforementioned resorufin dye. The distinction between the two emitters is wavelength of emission maximum (507 nm and 586 nm, respectively) and molecular size (Bodipy is a large pendant group, while resorufin is small and

initially thought to permeate through the pores). Samples of  $\beta$ -CDMOF-1 were loaded with each respective substrate in accordance with the above NMR analysis procedures, followed by crystal selection for microscopy. The samples were thoroughly rinsed to limit background fluorescence of free substrate and analyzed under a blanket of ethanol to prevent desolvation.

Quantitative analysis of  $\beta$ -CDMOF-1•BO-C reveals that emission properties of BO-C are more prominent on the crystal edges (*a*-axis) due to cumulative intensity of the higher fluorescence signal along the crystal edges (Figure 5a). Here, BO-C can bind on the surface by inclusion of the cholesterol portion, but not totally enter caused by the restrictive size of the Bodipy moiety. Intensity mapping illustrates this phenomenon with some emission intensity along the *b*-axis (crystal face), but with lower intensity, indication of a single layer (or lower cumulative concentration) of fluorophore. This image visually illustrates the surface inclusion of BO-C. Analysis of  $\beta$ -CDMOF-1•resorufin revealed quite different behaviour (Figure 5b). As noted in the NMR analysis, it was initially posited that the resorufin dye was of sufficient size to be included in the extended  $\beta$ -CD pores, however, this was not observed upon digestion of the MOF material. Confocal analysis revealed that that resorufin appears to permeate into the crystal fracture planes, which would presume to be areas of high polarity (opposite of what would be found inside the  $\beta$ -CD pores. Fluorescence intensity mapping revealed quite regular peak intensities across the crystal surface, indicative of dye being situated within the orthogonal crystal grain dislocations where the sugar oxides and potassium ions reside, rather than being restricted to the surface. This result nicely contrasts that of the inclusion of BO-C and further demonstrates the proclivity of cholesterol uptake in this unique system.

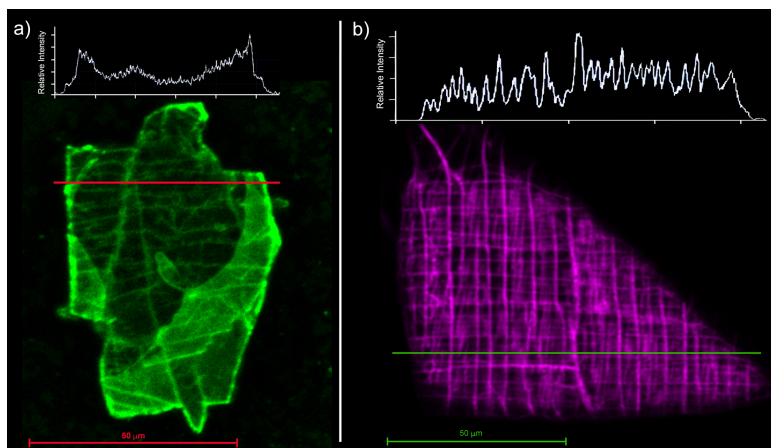


**Figure 5.** Confocal images of  $\beta$ -CDMOF-1 crystals loaded with a) Bodipy-cholesterol ( $\lambda_{\text{exc}} = 488$  nm, emission filters: BP 420-480 nm and BP 495-620 nm and b) resorufin dyes ( $\lambda_{\text{exc}} = 561$  nm, emission filters: BP 570-620 nm and LP 645 nm). Inset: fluorescence intensity profiles illustrating dye dispersion.

In conclusion, we have presented two new cyclodextrin-based MOFs employing  $\beta$ -CD as the structural building unit, one of which containing cholesterol within its pores. We also demonstrate that  $\beta$ -CDMOF-1 is capable of sterol uptake within its non-polar pores, and are able to contrast this behaviour with similarly-sized dye molecule that exhibited no uptake tendency. This work lays the foundation for our group to develop new MOF technologies related to extraction therapeutics, in this case, towards the combating of Atherosclerosis, and the potential for delivery of steroidal drugs.

## ASSOCIATED CONTENT

**Supporting Information.** The supporting information are available free of charge. In addition,

X-ray structural data has been uploaded to the Cambridge Crystallographic Database.

Experimental details with additional figures and tables (PDF)

X-ray data for  $\beta$ -CDMOF-1 (CCDC-1959832) and  $\beta$ -CDMOF-2•Chol (CCDC-1959833) (CIF)

## AUTHOR INFORMATION

### Corresponding Author

\*Email: [b.blight@unb.ca](mailto:b.blight@unb.ca)

### ORCID

Barry A. Blight [0000-0003-1166-6206](https://orcid.org/0000-0003-1166-6206)

Helena J. Shepherd [0000-0003-0832-4475](https://orcid.org/0000-0003-0832-4475)

Simon J. Teat [0000-0001-9515-2602](https://orcid.org/0000-0001-9515-2602)

Jeremy S. Rossman [0000-0001-6124-4103](https://orcid.org/0000-0001-6124-4103)

### Notes

The authors declare no competing financial interests.

## ACKNOWLEDGMENT

The authors are grateful for support from the University of Kent and the University of New Brunswick. TIA was funded by a University of Kent, School of Physical Science tuition scholarship and CSJ was funded by the New Brunswick Foundation for Innovation (NBIF) Research Assistant Initiative.

## REFERENCES

- (1) Rey-Rico, A.; Cucchiaroni, M. Supramolecular Cyclodextrin-Based Hydrogels for Controlled Gene Delivery. *Polymers (Basel)*. **2019**, *11* (3), 514–519.
- (2) Osman, S. K.; Brandl, F. P.; Zayed, G. M.; Teßmar, J. K.; Göpferich, A. M. Cyclodextrin Based Hydrogels: Inclusion Complex Formation and Micellization of Adamantane and Cholesterol Grafted Polymers. *Polymer (Guildf)*. **2011**, *52* (21), 4806–4812.
- (3) Schmidt, B.; Barner-Kowollik, C. Dynamic Macromolecular Material Design - The Versatility of Cyclodextrin Based Host/Guest Chemistry. *Angew. Chemie Int. Ed.* **2017**, 1–21.
- (4) Zhang, Y.-M.; Liu, Y.-H.; Liu, Y. Cyclodextrin-Based Multistimuli-Responsive Supramolecular Assemblies and Their Biological Functions. *Adv. Mater.* **2019**, *453*, 1806119–1806158.
- (5) Rajkumar, T.; Kukkar, D.; Kim, K.-H.; Sohn, J. R.; Deep, A. Cyclodextrin-Metal–Organic Framework (CD-MOF): From Synthesis to Applications. *J. Ind. Eng. Chem.* **2019**, *72*, 50–66.
- (6) Forgan, R. S.; Smaldone, R. A.; Gassensmith, J. J.; Furukawa, H.; Cordes, D. B.; Li, Q.; Wilmer, C. E.; Botros, Y. Y.; Snurr, R. Q.; Slawin, A. M. Z.; et al. Nanoporous Carbohydrate Metal–Organic Frameworks. *J. Am. Chem. Soc.* **2012**, *134* (1), 406–417.
- (7) Gassensmith, J. J.; Furukawa, H.; Smaldone, R. A.; Forgan, R. S.; Botros, Y. Y.; Yaghi, O. M.; Stoddart, J. F. Strong and Reversible Binding of Carbon Dioxide in a Green Metal–Organic Framework. *J. Am. Chem. Soc.* **2011**, *133* (39), 15312–15315.

- (8) Liu, Z.; Samanta, A.; Lei, J.; Sun, J.; Wang, Y.; Stoddart, J. F. Cation-Dependent Gold Recovery with  $\alpha$ -Cyclodextrin Facilitated by Second-Sphere Coordination. *J. Am. Chem. Soc.* **2016**, *138* (36), 11643–11653.
- (9) Liu, Z.; Frascioni, M.; Lei, J.; Brown, Z. J.; Zhu, Z.; Cao, D.; Iehl, J.; Liu, G.; Fahrenbach, A. C.; Botros, Y. Y.; et al. Selective Isolation of Gold Facilitated by Second-Sphere Coordination with  $\alpha$ -Cyclodextrin. *Nat. Commun.* **1AD**, *4*, 1855–1859.
- (10) Hartlieb, K. J.; Holcroft, J. M.; Moghadam, P. Z.; Vermeulen, N. A.; Algaradah, M. M.; Nassar, M. S.; Botros, Y. Y.; Snurr, R. Q.; Stoddart, J. F. CD-MOF: A Versatile Separation Medium. *J. Am. Chem. Soc.* **2016**, *138* (7), 2292–2301.
- (11) Yang, C.-X.; Zheng, Y.-Z.; Yan, X.-P.  $\gamma$ -Cyclodextrin Metal–Organic Framework for Efficient Separation of Chiral Aromatic Alcohols. *RSC Adv.* **2017**, *7* (58), 36297–36301.
- (12) Hartlieb, K. J.; Ferris, D. P.; Holcroft, J. M.; Kandela, I.; Stern, C. L.; Nassar, M. S.; Botros, Y. Y.; Stoddart, J. F. Encapsulation of Ibuprofen in CD-MOF and Related Bioavailability Studies. *Mol. Pharm.* **2017**, *14* (5), 1831–1839.
- (13) Sha, J.; Yang, X.; Sun, L.; Zhang, X.; Li, S.; Li, J.; Sheng, N. Unprecedented  $\alpha$ -Cyclodextrin Metal-Organic Frameworks with Chirality: Structure and Drug Adsorptions. *Polyhedron* **2017**, *127*, 396–402.
- (14) Ma, L.; Svec, F.; Lv, Y.; Tan, T. Engineering of the Filler/Polymer Interface in Metal–Organic Framework-Based Mixed-Matrix Membranes to Enhance Gas Separation. *Chem. - An Asian J.* **2019**, *311*, 614–639.

- (15) Zhang, Z.; Cano, Z. P.; Luo, D.; Dou, H.; Yu, A.; Chen, Z. Rational Design of Tailored Porous Carbon-Based Materials for CO<sub>2</sub> Capture. *J. Mater. Chem. A* **2019**, 7 (37), 20985–21003.
- (16) Hanikel, N.; Prévot, M. S.; Fathieh, F.; Kapustin, E. A.; Lyu, H.; Wang, H.; Diercks, N. J.; Glover, T. G.; Yaghi, O. M. Rapid Cycling and Exceptional Yield in a Metal-Organic Framework Water Harvester. *ACS Cent. Sci.* **2019**.
- (17) Wasson, M. C.; Buru, C. T.; Chen, Z.; Islamoglu, T.; Farha, O. K. Metal-Organic Frameworks: A Tunable Platform to Access Single-Site Heterogeneous Catalysts. *Appl. Catal. A Gen.* **2019**, 586 (May), 117214. <https://doi.org/10.1016/j.apcata.2019.117214>.
- (18) Koo, W.-T.; Jang, J.-S.; Kim, I.-D. Metal-Organic Frameworks for Chemiresistive Sensors. *Chem* **2019**, 1–26.
- (19) Yan, B. Photofunctional MOF-Based Hybrid Materials for the Chemical Sensing of Biomarkers. *J. Mater. Chem. C* **2019**, 7 (27), 8155–8175.
- (20) Zhang, Z.; Sang, W.; Xie, L.; Dai, Y. Metal-Organic Frameworks for Multimodal Bioimaging and Synergistic Cancer Chemotherapy. *Coord. Chem. Rev.* **2019**, 399, 213022.
- (21) zaro, I. A. nades L. Ã.; Forgan, R. S. Application of Zirconium MOFs in Drug Delivery and Biomedicine. *Coord. Chem. Rev.* **2019**, 380, 230–259.
- (22) Rabone, J.; Yue, Y. F.; Chong, S. Y.; Stylianou, K. C.; Bacsá, J.; Bradshaw, D.; Darling, G. R.; Berry, N. G.; Khimyak, Y. Z.; Ganin, A. Y.; et al. An Adaptable Peptide-Based

- Porous Material. *Science* (80) **2010**, 329 (5995), 1053–1057.
- (23) Martí-Gastaldo, C.; Warren, J. E.; Stylianou, K. C.; Flack, N. L. O.; Rosseinsky, M. J. Enhanced Stability in Rigid Peptide-Based Porous Materials. *Angew. Chemie Int. Ed.* **2012**, 51 (44), 11044–11048.
- (24) Katsoulidis, A. P.; Park, K. S.; Antypov, D.; Martí-Gastaldo, C.; Miller, G. J.; Warren, J. E.; Robertson, C. M.; Blanc, F.; Darling, G. R.; Berry, N. G.; et al. Guest-Adaptable and Water-Stable Peptide-Based Porous Materials by Imidazolate Side Chain Control. *Angew. Chemie Int. Ed.* **2013**, 53 (1), 193–198.
- (25) Huskic, I.; Pekov, I. V.; Krivovichev, S. V.; Friscic, T. Minerals with Metal-Organic Framework Structures. *Sci. Adv.* **2016**, 2 (8), e1600621–e1600621.
- (26) Smaldone, R. A.; Forgan, R. S.; Furukawa, H.; Gassensmith, J. J.; Slawin, A. M. Z.; Yaghi, O. M.; Stoddart, J. F. Metal-Organic Frameworks from Edible Natural Products. *Angew. Chemie Int. Ed.* **2010**, 49 (46), 8630–8634.
- (27) Sha, J.-Q.; Zhong, X.-H.; Wu, L.-H.; Liu, G.-D.; Sheng, N. Nontoxic and Renewable Metal–Organic Framework Based on  $\alpha$ -Cyclodextrin with Efficient Drug Delivery. *RSC Adv.* **2016**, 6 (86), 82977–82983.
- (28) Ohtani, Y.; Pitha, J.; Irie, T.; Uekama, K.; Fukunaga, K. Differential Effects of  $\alpha$ -,  $\beta$ - and  $\gamma$ -Cyclodextrins on Human Erythrocytes. *Eur. J. Biochem.* **1989**, 186, 17–22.
- (29) Rossman, J. S.; Jing, X.; Leser, G. P.; Lamb, R. A. Influenza Virus M2 Protein Mediates ESCRT-Independent Membrane Scission. *Cell* **2010**, 142 (6), 902–913.



- (30) Klein, U.; Gimpl, G.; Fahrenholz, F. Alteration of the Myometrial Plasma Membrane Cholesterol Content with  $\beta$ -Cyclodextrin Modulates the Binding Affinity of the Oxytocin Receptor. *Biochemistry* **1995**, *34* (42), 13784–13793.
- (31) Rothblat, G. H.; Christian, A. E.; Byun, H.-S.; Zhong, N.; Wanunu, M.; Marti, T.; Fürer, A.; Diedrich, F.; Bittman, R. Comparison of the Capacity of  $\beta$ -Cyclodextrin Derivatives and Cyclophanes to Shuttle Cholesterol between Cells and Serum Lipoproteins. *J. Lipid Res.* **1999**, *40*, 1475–1482.
- (32) Rothblat, G. H.; Christian, A. E.; Hayes, M. P.; Phillips, M. C. Use of Cyclodextrins for Manipulating Cholesterol Content. *J. Lipid Res.* **1997**, *38*, 2264–2272.
- (33) Kilsdonk, E. P.; Yancey, P. G.; Stoudt, G. W.; Bangerter, F. W.; Johnson, W. J.; Phillips, M. C.; Rothblat, G. H. Cellular Cholesterol Efflux Mediated by Cyclodextrins. *J. Biol. Chem.* **1995**, *270* (29), 17250–17256.
- (34) Selvidge, L. A.; Eftink, M. R. Spectral Displacement Techniques for Studying the Binding of Spectroscopically Transparent Ligands to Cyclodextrins. *Anal. Biochem.* **1986**, *154*, 400–408.
- (35) Christoforides, E.; Papaioannou, A.; Bethanis, K. Crystal Structure of the Inclusion Complex of Cholesterol in  $\beta$ -Cyclodextrin and Molecular Dynamics Studies. *Beilstein J. Org. Chem.* **2018**, *14*, 838–848.
- (36) Zhang, J.; Sun, H.; Ma, P. X. Host–Guest Interaction Mediated Polymeric Assemblies: Multifunctional Nanoparticles for Drug and Gene Delivery. *ACS Nano* **2010**, *4* (2), 1049–1059.

- (37) Liu, J.; Alvarez, J.; Ong, W.; Esteban Román, A.; Kaifer, A. E. *Phase Transfer of Hydrophilic, Cyclodextrin-Modified Gold Nanoparticles to Chloroform Solutions*; American Chemical Society, 2001.
- (38) Inokuma, Y.; Yoshioka, S.; Ariyoshi, J.; Arai, T.; Fujita, M. Preparation and Guest-Uptake Protocol for a Porous Complex Useful for “crystal-Free” Crystallography. *Nat. Protoc.* **2014**, 9 (2), 246–252.
- (39) Hölttä-Vuori, M.; Uronen, R.-L.; Repakova, J.; Salonen, E.; Vattulainen, I.; Panula, P.; Li, Z.; Bittman, R.; Ikonen, E. BODIPY-Cholesterol: A New Tool to Visualize Sterol Trafficking in Living Cells and Organisms. *Traffic* **2008**, 9 (11), 1839–1849.